

# Coarse and Fine Structure of the Pygmy Dipole Resonance

A P Tonchev<sup>1,2</sup>, S L Hammond<sup>3,2</sup>, J H Kelley<sup>4,2</sup>, E Kwan<sup>1,2</sup>,  
H Lenske<sup>5</sup>, R Raut<sup>1,2</sup>, G Rusev<sup>1,2</sup>, W Tornow<sup>1,2</sup>, and N Tsoneva<sup>5</sup>

<sup>1</sup> Duke University, Durham, North Carolina 27708-0308, USA

<sup>2</sup> Triangle Universities Nuclear Laboratory, Durham, North Carolina 27708-0308, USA

<sup>3</sup> University of North Carolina at Chapel Hill, Chapel Hill, North Carolina 27599-3255, USA

<sup>4</sup> North Carolina State University, Raleigh, North Carolina 27695-8202, USA

<sup>5</sup> Institut für Theoretische Physik, Universität Gießen, Gießen, D-35392, Germany

E-mail: tonchev@tunl.duke.edu

## Abstract.

High resolution and sensitivity studies of the nuclear dipole response in  $^{138}\text{Ba}$  have been performed in  $(\gamma, \gamma')$  experiment. The electric dipole character of the “pygmy” mode was experimentally verified for excitations from 4.0 to 8.5 MeV. Experimental findings have been compared with the quasiparticle phonon model. A new understanding about the character and the evolution of the pygmy resonance emerges from comparison of the experimental results with the theoretical calculations.

## 1. Introduction

Over the last decade, the low-energy  $E1$  strength in stable nuclei has been extensively studied in  $(\gamma, \gamma')$  scattering experiments below the maximum of the Giant Dipole Resonance (GDR) [3, 4, 5, 6, 7, 8, 9, 10, 11, 12, 13, 14]. These measurements were motivated by the observation of concentrated  $E1$  strength below the neutron-separation energy in semi-magic  $N = 50$  and 82 isotones, commonly referred to as the “pygmy” dipole resonance (PDR). The first theoretical calculations employing the three-fluid hydrodynamical model suggested that another type of dipole resonance might exist in the energy region below the GDR [15]. This low-energy dipole mode corresponds to the vibration of the neutron skin against the proton-neutron core with  $N \approx Z$ . Studies of the position and the distribution of the PDR have been carried out in the quasiparticle random-phase approximation (QRPA) incorporating multi-phonon extensions [17, 18]. These theoretical calculations suggested a correlation between the observed total  $B(E1)$  strength of the PDR and the neutron-to-proton ratio  $N/Z$  [17]. Analysis of transition densities describes clearly the specific features of this mode, making it distinct from the GDR. Additionally, it has been suggested that this excitation mode is independent of the type of nucleon excess (neutron or proton) [19], thereby defining it as a generic mode of excitation. However, these transition strengths account for only a few percent of the Thomas-Reiche-Kuhn (TRK) sum rule.

The observation of the PDR near the neutron separation energy may have important astrophysical implications. For example, it has been suggested that the nucleosynthesis of certain

neutron-deficient nuclei, the so-called  $p$  nuclei, is strongly influenced by PDR structures [20]. Pygmy resonance is an important topic of study at the new generation of radioactive ion beam facilities. Furthermore, important nuclear-structure effects have to be taken into account in order to interpret results obtained in the next generation of neutrinoless double-beta ( $0\nu\beta\beta$ ) decay experiments. Knowledge of the nuclear matrix elements, governed by the PDR, for example, will be indispensable for reliably deducing the effective Majorana mass [21].

The present report discusses completed photon-scattering measurements on  $^{138}\text{Ba}$  carried out using monoenergetic and 100% linearly-polarized photon beams from the High-Intensity Gamma-ray Source (HI $\gamma$ S) facility at Triangle Universities Nuclear Laboratory. These results are part of a continuing experimental activity at HI $\gamma$ S to study the nuclear dipole response in all stable  $N = 82$  nuclei.

## 2. Experimental Technique

The monoenergetic photon beams were produced by intra-cavity Compton backscattering of intense free-electron-laser light from electron beams in the Duke storage ring. The energy of the backward scattered photons can be tuned within a wide range, presently from about 1 MeV up to 100 MeV. The collimated photon flux on target exceeds  $1000 \gamma \text{ eV}^{-1} \text{ s}^{-1}$  within an energy spread of about 3%. More detailed information about HI $\gamma$ S facility can be found in Ref. [22].

The backscattered photons were collimated by a lead collimator of 30.5 cm in length with a cylindrical hole of 1.9 cm in diameter. After proper attenuation, the energy distribution of the photon beam was measured with a 123% HPGe detector placed in the beam. The photon flux was measured by Compton scattering of the beam from a 1.0-mm-thick copper plate, positioned 3 meters behind the barium target. Photons scattered from the copper plate through  $7.0^\circ \pm 1.6^\circ$  were detected with the same HPGe detector. At energies above 8.1 MeV, the photon flux was also monitored by the  $^{197}\text{Au}(\gamma, n)$  reaction.

The  $^{138}\text{Ba}$  target consisted of 4290.5 mg of  $\text{BaCO}_3$  powder enriched to 99.68% in  $^{138}\text{Ba}$ . It was placed into an evacuated plastic tube at the center of an array of five large-volume HPGe detectors. These detectors were arranged around the target at three positions:  $(\theta, \phi) = (90^\circ, 90^\circ)$  and  $(90^\circ, 270^\circ)$ ,  $(90^\circ, 0^\circ)$  and  $(180^\circ, 0^\circ)$ , and  $(135^\circ, 0^\circ)$ , where  $\theta$  is the polar angle with respect to the horizontally-polarized incoming photon beam, and  $\phi$  is the azimuthal angle measured from the polarization vector. This detector configuration, shown in Fig. 1, allows for the unambiguous determination of  $E1$ ,  $M1$ , and  $E2$  transitions in any nucleus, regardless of the spin of its ground state.

The Nuclear Resonance Fluorescence method (NRF) is used at HI $\gamma$ S to study low-multipolarity ground-state transitions i.e.,  $E1$ ,  $M1$  and to a lesser extent  $E2$  with large partial widths [23, 24]. The NRF technique with an established high-detection sensitivity represents an outstanding tool for measuring dipole transitions. The main advantage of this method is that both the excitation and the de-excitation processes proceed via the electromagnetic interaction, which is the most understood fundamental interaction in physics. The angular distribution of the scattered  $\gamma$  rays from excited nuclei to the ground state or to other excited levels are measured with large volume HPGe detectors positioned at different angles relative to the incoming linearly-polarized photon beam.

## 3. Experimental Results

Three gamma-ray spectra from the  $^{138}\text{Ba}$  target at three different photon energies,  $E_\gamma = 5.4$ , 7.2, and 8.5 MeV, are shown in Figures 2 and 3. The low-energy part of the scattering spectra is shown in Fig. 2, while the high-energy part, beneath the photon beam, is shown in Fig. 3. Spectra in blue are those  $\gamma$  rays observed in the vertical detectors, while spectra in red are those observed in the horizontal detectors. The  $\gamma$ -ray peaks under the beam energies represent specific ground-state transitions. These ground-state transitions appear mainly in the vertical

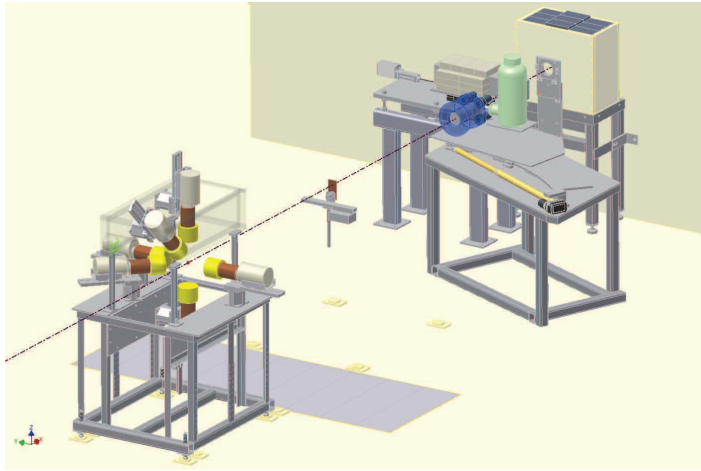


**Figure 1.** The detector setup at HIγS facility.

plane  $(\theta, \phi) = (90^\circ, 90^\circ \text{ and } 270^\circ)$  with respect to the initial linearly-polarized photon beam. The ground-state transitions account for the larger contribution in the elastic-scattering process in this closed-shell nucleus. The increased complexity of the scattered  $\gamma$ -ray spectra with photon energy can be seen from Fig. 3. At excitation energies closer to the neutron separation energy, unresolved peak strengths have to be taken into account. The increased population of the first three  $2^+$  states with photon energies is shown in Fig. 2. These  $2^+_{1,2,3}$  states are populated by  $\gamma$  transitions from the beam energy and are quantitative measure of the inelastic cross-section process. The unresolved strength was evaluated when the detector response was folded into the data. It was estimated that the unresolved dipole strength near the neutron separation energy is about one quarter of the total photoabsorption strength.

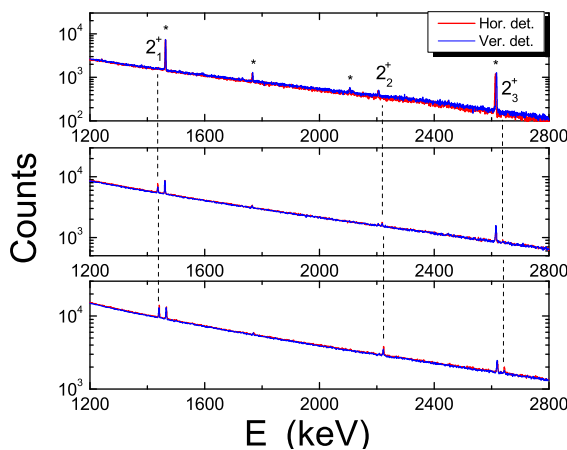


**Figure 2.** Low-energy part of the photon scattered spectra from  $^{138}\text{Ba}$  at  $E_\gamma = 5.4$  (top),  $7.2$  (middle), and  $8.5$  (bottom) MeV.

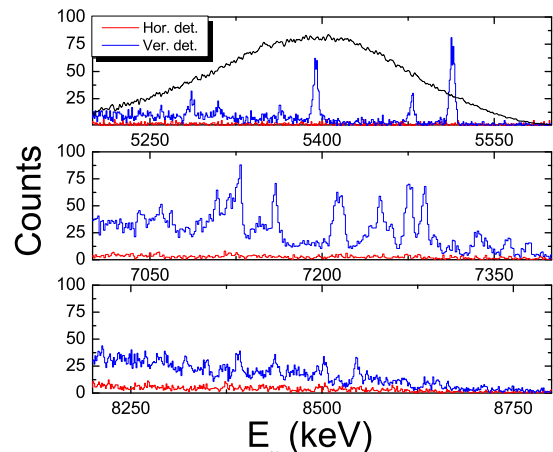


**Figure 3.** High-energy part of the photon scattered spectra from  $^{138}\text{Ba}$  at  $E_\gamma = 5.4$  (top),  $7.2$  (middle), and  $8.5$  (bottom) MeV.

Figure 4 shows the azimuthal asymmetry  $A_s = (I_H - I_V)/(I_H + I_V)$ , where  $I_H$  and  $I_V$  are the intensities in the horizontal and vertical detectors, respectively, measured for 150 dipole transitions ( $E1$  and  $M1$ ) observed in  $^{138}\text{Ba}$ . Our measurements confirmed the previous parity assignment at HIγS between 5.5 and 6.5 MeV [6] and the dipole character of the states measured

in Refs. [3, 10]. However, our higher experimental sensitivity allowed us to observe 87 new dipole states in  $^{138}\text{Ba}$ . Most of these states are located at energies above 6.5 MeV and each has relatively small strength. The summed  $E1$  transition strength from 4.0 to 8.5 MeV is  $\Sigma B(E1)\uparrow = 0.96(18) e^2 fm^2$  corresponds to 1.25% of the TRK sum rule. It should be noted that the remaining asymmetry is observed for the secondary  $\gamma$  transitions connecting the  $2_{1,2,3}^+$  states with the ground state. This asymmetry shows peculiar energy dependence with maximum values of  $As = + 0.20(3)$  at excitation energy around 6.5 MeV.

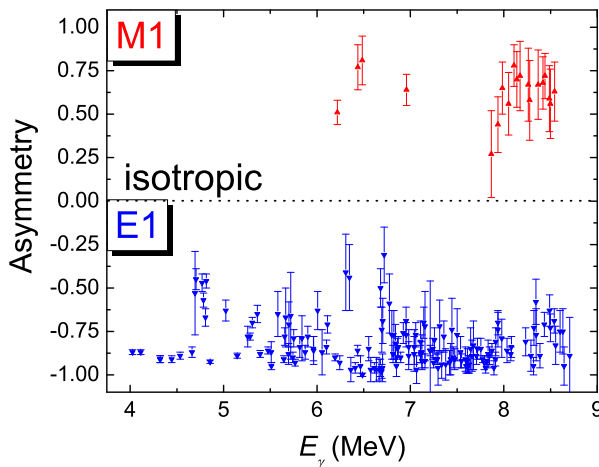


**Figure 4.** The measured asymmetry of the  $M1$  (top panel) and  $E1$  (bottom panel) transitions in  $^{138}\text{Ba}$  from 4 to 8.5 MeV.

The elastic ( $\sigma_{\gamma\gamma}$ ), inelastic ( $\sigma_{\gamma\gamma'}$ ), and photoabsorption ( $\sigma_{\gamma} = \sigma_{\gamma\gamma} + \sigma_{\gamma\gamma'}$ ) cross section for the  $^{138}\text{Ba}(\bar{\gamma},\gamma')$  reaction below the neutron-separation energy is shown in the upper panel of Fig. 5 [25]. These cross sections include transitions from both  $1^-$  and  $1^+$  states. The elastic cross section, derived from ground-state transitions, shows resonance-like structures. In contrast, the inelastic cross section which arises from statistical decays, shows an exponential increase with excitation energy. The deduced photoabsorption cross section ( $\sigma_{\gamma}$ ) in comparison to the experimental data for the  $^{138}\text{Ba}(\gamma,xn)$  reaction in the GDR region [26] is shown in the lower panel of Fig. 5. As can be seen, for energies below the neutron separation energy ( $S_n$ ) the photoabsorption cross section has values larger than the extrapolation of the tail of the GDR implies.

#### 4. Theoretical calculations

The full QPM calculations, which account for non-harmonic effects, are important for reproducing the fragmentation pattern below the neutron separation energy. In Fig. 6 we present our QPM results in comparison with the present experimental data for the  $1^{\pm}$  states in  $^{138}\text{Ba}$  at  $E^* < 8.5$  MeV. The  $M1$  transitions in  $^{138}\text{Ba}$  do not manifest obvious resonance or distinct structures of the type exhibited by  $E1$  states below the neutron separation energy. The  $E1$  PDR is broad and characterized by a high level density. In contrast, the magnetic dipole transitions are more isolated. The  $1^-$  QRPA states are fragmented over a large number of multi-phonon states below  $E^* = 8.5$  MeV. In the PDR region, the QPM calculations predict for the direct  $E1$  ground-state transitions the summed strength  $\Sigma B(E1)\uparrow = 1.22 e^2 fm^2$  with a centroid energy  $\bar{E}^* = 7.3$  MeV. These values compare very well with the present measurements: summing over the experimentally observed  $1^-$  states, one finds  $\Sigma B_{exp}(E1)\uparrow = 0.96 e^2 fm^2$  and  $\bar{E}_{exp}^* = 6.7$  MeV. From analysis of dipole transition densities the observed  $E1$  strength at

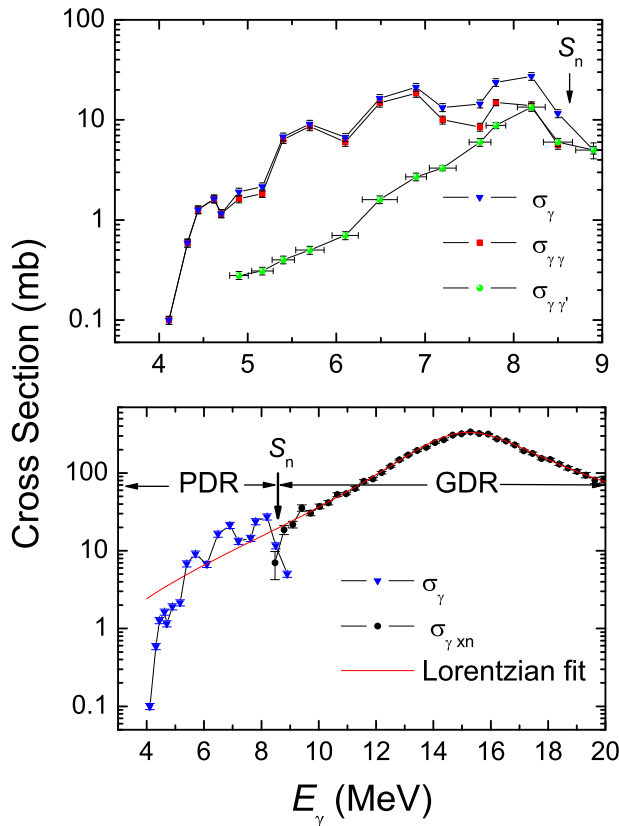


**Figure 5.** Upper panel: Elastic ( $\sigma_{\gamma\gamma}$ ), inelastic ( $\sigma_{\gamma\gamma'}$ ), and total absorption cross sections ( $\sigma_{\gamma}$ ) in  $^{138}\text{Ba}$  below the one-neutron separation energy ( $S_n=8.6$  MeV) and averaged over energy bins of about 0.3 MeV. Lower panel: Total absorption cross section ( $\sigma_{\gamma}$ ) from the present photon-scattering experiment in comparison with  $(\gamma, xn)$  data [26]. A Lorentzian curve is applied to the experimental photoneutron cross-section data.

$E^* < 8.5$  MeV is related to neutron skin oscillations and PDR mode [25]. Even though some admixtures of low-energy isovector excitations of the GDR contribute to the substantial increase of the E1 strength at  $E^* > 8$  MeV.

## 5. Conclusion

The systematic spin and parity measurements on  $^{138}\text{Ba}$  at the HI $\gamma$ S facility have verified for the first time that the observed dipole strength from 4 MeV to the neutron separation energy is predominantly of electric dipole nature. Our findings are in agreement with the QPM prediction for the character and strength of this dipole excitation mode. Enhanced dipole strength above the Lorentzian extrapolation of the GDR has been directly measured for elastic and inelastic transitions below the neutron separation energy. The deduced photoabsorption cross section  $\sigma_{\gamma}$  exhibits a resonance-like shape distribution with pronounced peak structure. In addition, the fine structure of the  $M1$  “spin-flip” mode was observed for the first time in  $N = 82$  nuclei. These results reveal the interplay between the GDR and the PDR. The low-energy (below 6.5 MeV) PDR exhibits a mostly isoscalar excitation mode. As the excitation energy increases, the isovector contribution to the dipole strength increases exponentially due to the presence of the low-energy tail of the GDR.

## Acknowledgments

We are grateful to the HI $\gamma$ S facility staff for their assistance in delivering excellent photon beams. This research was supported by the DOE grants DE-FG02-97ER41033, DE-FG02-97ER41041, DE-FG02-97ER41042, DE-FG52-09NA29448, and DFG grant Le439/6.

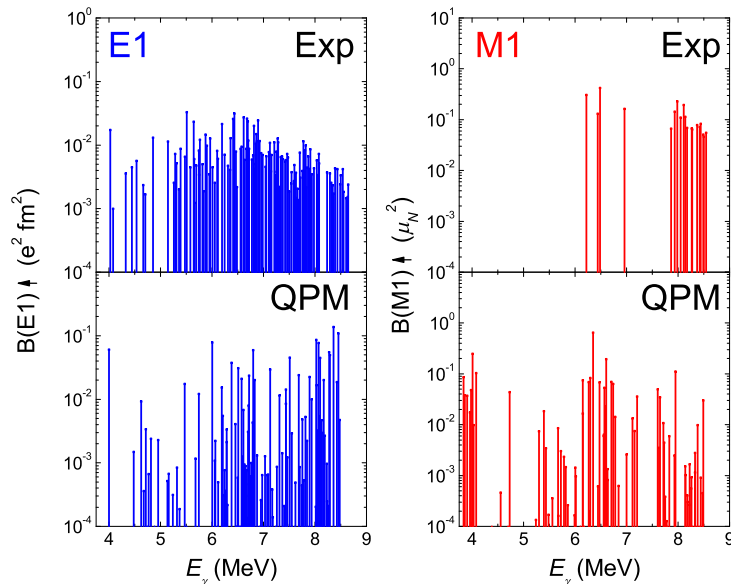


**Figure 6.** Experimental results (top panels) and the QPM calculations (bottom panels) of direct transitions to the  $1^-$  (left panels) and  $1^+$  (right panels) excited states located below the neutron separation energy in  $^{138}\text{Ba}$ .

## References

- [1] Strite S and Morkoc H 1992 *J. Vac. Sci. Technol. B* **10** 1237
- [2] Jain S C, Willander M, Narayan J and van Overstraeten R 2000 *J. Appl. Phys.* **87** 965
- [3] Herzberg R -D *et al.* 1999 *Phys. Rev. C* **60** 051307
- [4] Ryezayeva N *et al.* 2002 *Phys. Rev. Lett.* **89** 272502
- [5] Zilges A *et al.* 2002 *Phys. Lett. B* **542** 43
- [6] Pietralla N *et al.* 2001 *Phys. Rev. Lett.* **88** 012502
- [7] Käubler L *et al.* 2004 *Phys. Rev. C* **70** 064307
- [8] Enders E *et al.* 2004 *Nucl. Phys. A* **741** 3
- [9] Adrich P *et al.* 2005 *Phys. Rev. Lett.* **95** 132501
- [10] Voltz S *et al.* 2006 *Nucl. Phys. A* **779** 1
- [11] Savran D *et al.* 2006 *Phys. Rev. Lett.* **97** 172502
- [12] Rusev G *et al.* 2006 *Eur. Phys. J. A* **76** 171
- [13] Schwengner R *et al.* 2008 *Phys. Rev. C* **78** 064314
- [14] Savran D *et al.* 2008 *Phys. Rev. Lett.* **100** 232501
- [15] Mohan R *et al.* 1971 *Phys. Rev. C* **3** 1740
- [16] Suzuki Y *et al.* 1990 *Prog. Theor. Phys.* **83** 180
- [17] Tsoneva N, Lenske H 2004 *Phys. Lett. B* **586** 213
- [18] Tsoneva N, Lenske H 2008 *Phys. Rev. C* **77** 024321
- [19] Paar N *et al.* 2005 *Phys. Rev. Lett.* **94** 182501
- [20] Arnould M, Goriely S 2003 *Phys. Rep.* **384** 1
- [21] Suhonen J *et al.* 2008 *Phys. Lett. B* **668** 277
- [22] Weller H R *et al.* 2009 *Prog. Part. Nucl. Phys.* **62** 257
- [23] Kneissl U *et al.* 1996 *Prog. Part. Nucl. Phys.* **37** 349
- [24] Kneissl U *et al.* 2006 *J. Phys. G: Nucl. Part. Phys.* **32** R217
- [25] Tonchev A P *et al.* 2010 *Phys. Rev. Lett.* **104** 072501
- [26] Berman B L *et al.* 1970 *Phys. Rev. C* **2** 2318